

Limited brain distribution of Ro 64-0802, a pharmacologically active form of oseltamivir, by active efflux across the blood–brain barrier mediated by organic anion transporter 3 (Oat3/*Slc22a8*) and multidrug resistance-associated protein 4 (Mrp4/*Abcc4*)

Atsushi Ose, Mototsugu Ito, Hiroyuki Kusuhara, Kenzo Yamatsugu, Motomu Kanai, Masakatsu Shibasaki, Masakiyo Hosokawa, John D. Schuetz, Yuichi Sugiyama

Graduate School of Pharmaceutical Sciences, The University of Tokyo, Bunkyo-ku, Tokyo, Japan
(A.O., M.I., H.K., K.Y., M.K., M.S., Y.S.)

Chiba Institute of Science, Choshi-city, Chiba, Japan (M.H.)

Department of Pharmaceutical Sciences, St. Jude Children's Research Hospital, Memphis, Tennessee
(J.S.)

Running title: Active efflux of Ro 64-0802 by Mrp4 and Oat3 at the BBB

Corresponding author: Yuichi Sugiyama

Address:

Department of Molecular Pharmacokinetics,

Graduate School of Pharmaceutical Sciences,

The University of Tokyo

7-3-1 Hongo, Bunkyo-ku, Tokyo 113-0033, Japan

Phone : +81-3-5841-4770 Fax : +81-3-5841-4767

E-mail : sugiyama@mol.f.u-tokyo.ac.jp

Number of Text Pages: 25

Figures: 7

References: 40

Number of Words: Abstract, 244

Introduction, 753

Discussion, 1166

Abbreviations

BBB, blood–brain barrier; P-gp, P-glycoprotein; Bcrp, breast cancer resistance protein; Mrp, multidrug resistance-associated protein; Oat, organic anion transporter; Oatp, organic anion transporter peptide; CES, carboxylesterase; $K_{p,brain}$, brain-to-plasma concentration ratio

Abstract

Ro 64-0802 is a pharmacologically active form of the anti-influenza virus drug oseltamivir. Abnormal behavior is a suspected adverse effect of oseltamivir on the central nervous system. This study focused on the transport mechanisms of Ro 64-0802 across the blood–brain barrier (BBB). Ro 64-0802 was found to be a substrate of OAT3/*SLC22A8* and MRP4/*ABCC4*. HEK293 cells expressing OAT3 exhibited a greater intracellular accumulation of Ro 64-0802 than mock-transfected cells (15 *versus* 1.2 $\mu\text{L}/\text{mg}$ protein/10 min, respectively). The efflux of Ro 64-0802 was three fold greater when MRP4 was expressed in MDCKII cells, and was significantly inhibited by indomethacin. Following its microinjection into the cerebrum, the amount of Ro 64-0802 in brain was significantly greater in both *Oat3*^{-/-} mice and *Mrp4*^{-/-} mice compared with the corresponding wild-type mice (0.36 *versus* 0.080, and 0.32 *versus* 0.060 nmol at 120 min after injection, respectively). The brain-to-plasma concentration ratio ($K_{p,\text{brain}}$) of Ro 64-0802, determined in wild-type mice after subcutaneous continuous infusion for 24 h, was close to the capillary volume (ca. 10 $\mu\text{L}/\text{g}$ brain). Although the $K_{p,\text{brain}}$ of Ro 64-0802 was unchanged in *Oat3*^{-/-} mice, it was significantly greater in *Mrp4*^{-/-} mice (41 $\mu\text{L}/\text{g}$ brain). These results suggest that Ro 64-0802 can cross the BBB from the blood, but its brain distribution is limited by its active efflux by Mrp4 and Oat3 across the BBB. The transporter responsible for the brain uptake of Ro 64-0802 remains unknown, but Oat3 is a candidate transporter.

Introduction

Oseltamivir is an ester-type prodrug of Ro 64-0802, a potent and selective inhibitor of viral neuraminidase, a key enzyme involved in the release of influenza virus from the host cells. Oseltamivir is used for the treatment and prophylaxis of infectious diseases caused by both Influenzavirus A and Influenzavirus B (Bardsley-Elliot and Noble, 1999). Recently, abnormal behavior, such as jumping and falling from balconies, has been reported in teenagers or younger people prescribed oseltamivir (<http://www.fda.gov/cder/drug/infopage/tamiflu/QA20051117.htm>; (Fuyuno, 2007). In response to these reports, the Ministry of Health, Labor and Welfare has issued a warning regarding the use of oseltamivir as a medication for teenagers or younger people and has prohibited the prescription of oseltamivir for them in Japan.

Several animal studies have reported the pharmacological actions of oseltamivir on the central nervous system (Izumi et al., 2007; Satoh et al., 2007; Usami et al., 2008; Yoshino et al., 2008), although the association between such pharmacological actions and abnormal behavior remains an open question. The systemic administration of oseltamivir increases dopamine levels in the rat medial prefrontal cortex (Yoshino et al., 2008), and oseltamivir and Ro 64-0802 enhance spike synchronization between hippocampal CA3 pyramidal cells and evoked synchronized population bursts, which recruit virtually all the neurons in the network (Usami et al., 2008). It has also been demonstrated that oseltamivir and Ro 64-0802 affect neuronal excitability in rat hippocampal slices and that Ro 64-0802 is 30 times more potent than oseltamivir (Izumi et al., 2007).

Whether oseltamivir and Ro 64-0802 cross the blood–brain barrier (BBB) is an important issue considering their pharmacological actions on the central nervous system. In clinical studies, both oseltamivir and Ro 64-0802 were detected in the plasma following the oral administration of oseltamivir. Oseltamivir is converted to Ro 64-0802 by carboxylesterase 1A1 (CES1A1) in the liver (Shi et al., 2006). Most of the administered dose is recovered in the urine as Ro 64-0802 by glomerular filtration and tubular secretion by organic anion transporters in the kidney (He et al., 1999). The penetration of drugs to the brain from the circulating blood is limited by the BBB, which is formed by endothelial cells connected tightly to adjacent cells. It has been shown that oseltamivir can cross

the BBB, but P-glycoprotein (P-gp) limits its brain penetration at the BBB (Morimoto et al., 2008; Ose et al., 2008). In contrast, Ro 64-0802 exhibits only a limited distribution in the brain because it is close to the brain capillary volume. Therefore, the permeability of Ro 64-0802 across the BBB has been considered to be quite low because of its hydrophilic nature and anionic charge at neutral pH.

In this study, we hypothesized that the low distribution of Ro 64-0802 in the brain is attributable to active efflux at the BBB. We focused on two organic anion transporters—organic anion transporter 3 (OAT3/*SLC22A8*) and multidrug resistance-associated protein 4 (MRP4/*ABCC4*)—as the candidate transporters involved. Oat3 is expressed on the abluminal membrane of the brain capillary endothelial cells in rodents (Kikuchi et al., 2003; Mori et al., 2003; Roberts et al., 2008). Cumulative in vivo studies suggest that Oat3 plays a significant role in the uptake of hydrophilic organic anions into the endothelial cells, the first step in its overall elimination from the brain to the blood (Ohtsuki et al., 2002; Kikuchi et al., 2003; Mori et al., 2003; Kikuchi et al., 2004; Mori et al., 2004). Ro 64-0802 has been identified as a substrate of OAT1/*SLC22A6* (Hill et al., 2002). Considering the overlapping substrate specificities of OAT1 and OAT3, it is possible that OAT3 accepts Ro 64-0802 as substrate. MRP4 is an ABC transporter localized in the luminal membrane of the brain capillary endothelial cells (Leggas et al., 2004). MRP4 accepts anionic drugs as substrates (Ci et al., 2007; Hasegawa et al., 2007; Imaoka et al., 2007) and mediates their unidirectional efflux into the circulating blood (Leggas et al., 2004). It has been demonstrated that the elimination of topotecan from the brain was delayed and that the concentration of topotecan in the cerebrospinal fluid was greatly enhanced in *Mrp4*^{-/-} mice compared with the corresponding wild-type mice (Leggas et al., 2004). It has been also demonstrated that the brain-to-plasma concentration ratio of 9'-(2'-phosphonylmethoxyethyl)-adenine 3h after intravenous administration was greater in *Mrp4*^{-/-} mice than in wild-type mice (Belinsky et al., 2007).

In this study, in vivo experiments were undertaken using wild-type, *Oat3*^{-/-}, and *Mrp4*^{-/-} mice to examine the involvement of Oat3 and Mrp4 in the uptake and efflux of Ro 64-0802 across the BBB.

Materials and Methods

Reagents

Oseltamivir phosphate and its active metabolite, Ro 64-0802 (purity; >95%), were synthesized according to a previous report (Yamatsugu et al., 2007). All other chemicals used in the experiments were of analytical grade.

Animals

Mrp4^{-/-} mice had been established previously (Leggas et al., 2004). *Oat3*^{-/-} mice were obtained from Deltagen (San Carlos, CA, USA). Male C57BL/6J, *Mrp4*^{-/-}, and *Oat3*^{-/-} mice were maintained by CLEA Japan, Inc. (Tokyo, Japan). All mice (10–18 weeks old) were maintained under standard conditions with a reverse dark–light cycle. Food and water were available ad libitum. All experiments using animals in this study were carried out according to the guidelines provided by the Institutional Animal Care Committee (Graduate School of Pharmaceutical Sciences, University of Tokyo).

Uptake of Ro 64-0802 by human OAT3-expressing human embryonic kidney (HEK) 293 cells

An in vitro transport experiment was carried out as described previously (Deguchi et al., 2004). After the cells had been washed twice and preincubated with Krebs–Henseleit buffer at 37 °C for 15 min, drug uptake was initiated by the addition of Krebs–Henseleit buffer containing Ro 64-0802 (10 μM). The Krebs–Henseleit buffer consisted of 118 mM NaCl, 23.8 mM NaHCO₃, 4.8 mM KCl, 1.0 mM KH₂PO₄, 1.2 mM MgSO₄, 12.5 mM HEPES, 5.0 mM glucose, and 1.5 mM CaCl₂, adjusted to pH 7.4. Uptake was terminated at the designated times by the addition of ice-cold Krebs–Henseleit buffer after the removal of the incubation buffer. The cells were then washed twice with 1 mL of ice-cold Krebs–Henseleit buffer, solubilized in 500 μL of 1 mM Tris-HCl buffer (pH 7.4), and stored overnight at 4 °C. After sonication, aliquots (250 μL) were subjected to liquid chromatography–mass spectrometry (LC–MS) analysis. The remaining 20 μL of cell lysate was used to determine the protein concentration with the method of Lowry, with bovine serum albumin (BSA) as the standard.

Construction of human MRP4/CES1A1-expressing MDCKII cells

CES1A1 cDNA was subcloned into the pTARGET vector (Promega, Madison, WI, USA) (Mori et al., 1999) and transfected into Madin–Darby canine kidney (MDCK) II cells with lipofectamine 2000 reagent (Invitrogen, Carlsbad, CA, USA), according to the manufacturer's protocol. The transfectants were selected by culturing them in the presence of neomycin (1600 µg/mL) (Invitrogen) and were maintained in Dulbecco's modified Eagle's medium (Gibco) supplemented with 10% fetal bovine serum, 1% antibiotic–antimycotic (Gibco), and neomycin (400 µg/mL) at 37 °C with 5% CO₂ and 95% humidity. MDCKII cells with sufficient CES1A1 activity (CES1A1-MDCKII) were cloned and used as the hosts for infection with recombinant adenovirus carrying the human MRP4 gene, which had been established previously (Ci et al., 2007; Hasegawa et al., 2007; Imaoka et al., 2007). CES1A1-MDCKII cells were infected with recombinant adenovirus containing human MRP4 transporter cDNA at a multiplicity of infection of 10 for 48 h to overexpress human MRP4 (MRP4/CES1A1-MDCKII). Green fluorescent protein (GFP) was used as the negative control (GFP/CES1A1-MDCKII).

The expression of MRP4 protein was confirmed by western blotting. The cell lysates were loaded onto a sodium dodecyl sulfate (SDS) polyacrylamide gel (7.5%) with a 3.75% stacking gel. N-Linked carbohydrate groups were cleaved from the MRP4 protein in the cell lysates with PNGase F (N-glycosidase F; New England Biolabs, Inc., Beverly, MA, USA). Digestion was performed according to the manufacturer's instructions, except that the samples were incubated for 30 min at 37 °C in denaturing buffer rather than for the recommended 10 min at 100 °C. To minimize protein degradation, protease inhibitors were included in all the steps. After incubation at 37 °C for 30 min, the samples were separated by SDS–polyacrylamide gel (7.5%) electrophoresis (PAGE). The proteins were electroblotted onto a polyvinylidene difluoride membrane (Pall, Port Washington, NY, USA). The membrane was blocked with blocking buffer (Tris-buffered saline containing 0.05% Tween 20 (TTBS) and 3% skimmed milk) for 1 h at room temperature. After it had been washed with TTBS, the membrane was incubated overnight at 4 °C with monoclonal anti-MRP4 M4I-10 antibody (1:1000 in blocking buffer; Abcam). The protein was detected by binding

horseradish-peroxidase-labeled anti-rat IgG antibody (1:5000 in blocking buffer; Amersham Bioscience). Immunoreactivity was detected with an ECL Plus Western Blotting Detection Kit (Amersham Biosciences).

Efflux of Ro 64-0802 formed intracellularly from oseltamivir in MRP4/CES1A1-MDCKII and GFP/CES1A1-MDCKII cells

After the cells had been washed twice and preincubated with Krebs–Henseleit buffer at 37 °C for 15 min, oseltamivir (10 μM) was added to the incubation buffer in the presence or absence of indomethacin (50 μM). At the designated times, the incubation buffer was collected. Ice-cold Krebs–Henseleit buffer was then added, and the cells were washed four times. After the cells had been collected, they were frozen in liquid nitrogen and stored at –80 °C until use. The efflux clearance of Ro 64-0802 from the transfectants was determined using the integration plot method. The amount of Ro 64-0802 effluxed to the buffer at time t [$X_{\text{buffer}}(t)$, nmol/mg protein] can be described by the following equation:

$$dX_{\text{buffer}}(t)/dt = CL_{\text{efflux}} \times C_{\text{cell}}(t) \quad (1)$$

where CL_{efflux} (μL/min per mg protein) represents the efflux clearance of Ro 64-0802 from the cells, and $C_{\text{cell}}(t)$ (μM) is the cellular concentration of Ro 64-0802. Cellular volume was assumed to be 4 μL/mg protein. The integration of this equation from time 0 to time t yields the following equation:

$$X_{\text{buffer}}(t) = CL_{\text{efflux}} \times \text{AUC}_{\text{cell}}(0-t) \quad (2)$$

where $\text{AUC}_{\text{cell}}(0-t)$ (μM × min) represents the area under the cellular concentration–time curve for Ro 64-0802 from time 0 to time t . Because the amount of Ro 64-0802 in buffer [$A_{\text{buffer}}(t)$, nmol/mg protein] is given by the sum of $X_{\text{buffer}}(t)$ and the amount of Ro 64-0802 existing in the buffer at time 0 (X_0), $A_{\text{buffer}}(t)$ is described by the following equation:

$$A_{\text{buffer}}(t) = CL_{\text{efflux}} \times \text{AUC}_{\text{cell}}(0-t) + X_0 \quad (3)$$

Thus, the CL_{efflux} value can be obtained by fitting $A_{\text{buffer}}(t)$ versus $AUC_{\text{cell}}(0-t)$ using a least-squares regression program (MULTI) (Yamaoka et al., 1981).

Efflux of Ro 64-0802 from the cerebral cortex of wild-type, *Oat3*^{-/-} and *Mrp4*^{-/-} mice following microinjection

The efflux of the test compounds from the brain after their microinjection into the cerebral cortex was investigated using the brain efflux index method, as described previously (Kakee et al., 1996). Ro 64-0802 (1 mM) in 0.5 μL of ECF buffer (122 mM NaCl, 25 mM NaHCO_3 , 10 mM D-glucose, 3 mM KCl, 1.4 mM CaCl_2 , 1.2 mM MgSO_4 , 0.4 mM K_2HPO_4 , and 10 mM HEPES, pH 7.4) was injected into the cerebral cortex (4.5 mm lateral to the bregma, 2.5 mm in depth). After the intracerebral microinjection, the mice were decapitated, and the amount of Ro 64-0802 that remained in the ipsilateral cerebrum was determined with LC-MS analysis.

Brain-to-plasma concentration ratio of Ro 64-0802 following subcutaneous infusion of oseltamivir or Ro 64-0802 in wild-type, *Oat3*^{-/-} and *Mrp4*^{-/-} mice

Male C57BL/6J mice, *Mrp4*^{-/-} mice, and *Oat3*^{-/-} mice (10–18 weeks old), weighing approximately 25–30 g, were used for these experiments. An osmotic pump (8 $\mu\text{L}/\text{h}$; Alzet) was implanted under the skin in the backs of the mice under pentobarbital anesthesia (30 mg/kg). The mice received a continuous subcutaneous infusion of oseltamivir or Ro 64-0802 at doses of 400 nmol/h per mouse or 80 nmol/h per mouse, respectively. Blood samples were collected from the postcaval vein at 24 h after treatment under pentobarbital anesthesia, and the brain was excised immediately. Plasma was obtained by centrifugation of the blood samples (10,000 $\times g$). The esterase inhibitor, dichlorvos (200 $\mu\text{g}/\text{mL}$), was used to prevent ex vivo hydrolysis of the oseltamivir to Ro 64-0802 in the blood and plasma (Wiltshire et al., 2000; Lindegardh et al., 2006). The plasma and brain concentrations of Ro 64-0802 were determined with LC-MS analysis.

Quantification of Ro 64-0802 in plasma and brain specimens

The brain was homogenized with a fourfold volume of phosphate-buffered saline to obtain a 20% brain homogenate. Plasma specimens (10 μ L) were mixed with 40 μ L of ethanol, and the brain homogenates (100 μ L) were mixed with 400 μ L of ethanol. All these mixed solutions were centrifuged at $15,000 \times g$ for 10 min. The supernatants of the plasma specimens were mixed with an equal volume of water and subjected to LC–MS analysis. The supernatants of the brain specimens (350 μ L) were evaporated, and the pellets were reconstituted with 50 μ L of 20% ethanol. The reconstituted specimens were centrifuged at $15,000 \times g$ for 10 min, and an aliquot of the supernatant was subjected to LC–MS analysis.

An LCMS2010EV equipped with a Prominence LC system (Shimadzu, Kyoto, Japan) was used for the analysis. Samples were separated on a CAPCELL PAK C18 MGII column (3 μ m, 2 mm \times 50 mm; Shiseido, Tokyo, Japan) in binary gradient mode at a flow rate of 1 mL/min. Formic acid (0.05%) and acetonitrile were used for the mobile phase. The acetonitrile concentration was initially 10%, and then increased linearly to 40% over 2 min. Finally, the column was reequilibrated at an acetonitrile concentration of 10% for 3 min. The total run time was 5 min. Ro 64-0802 was eluted at 2.5 min. In the mass analysis, Ro 64-0802 was detected at a mass-to-charge ratio of 285.15 under positive electron spray ionization conditions. The interface voltage was -3.5 kV, and the nebulizer gas (N_2) flow was 1.5 L/min. The heat block and curved desolvation line temperatures were 200 $^{\circ}$ C and 150 $^{\circ}$ C, respectively.

Statistical analysis

Data are presented as the means \pm standard errors (SE) of 3–6 animals, unless otherwise specified. Student's two-tailed unpaired t test and one-way ANOVA followed by Tukey's multiple comparison test were used to identify significant differences between groups when appropriate. Statistical significance was set at $P < 0.05$.

Results

Uptake of Ro 64-0802 into human OAT3-expressing HEK293 cells

To show that Ro 64-0802 is an OAT3 substrate, an in vitro transport experiment was performed. The intracellular accumulation of Ro 64-0802 was significantly greater in HEK293 cells expressing human OAT3 than in mock-transfected cells (1.2 ± 0.2 and 15.1 ± 0.2 $\mu\text{L}/10$ min per mg protein for vector-transfected and OAT3-expressing HEK293 cells, respectively).

Construction of human MRP4/CES1A1-expressing MDCKII cells

A clone of the MDCKII cells exogenously expressing CES1A1 was selected by measuring the hydrolytic activity against *p*-nitrophenyl acetate (data not shown). The subsequent study was performed using this clone as the host. After infection with the recombinant adenovirus, the protein expression of MRP4 in the MRP4/CES1A1-expressing MDCKII cells was confirmed by western blot analysis (Fig. 1A). An anti-MRP4 monoclonal antibody recognized a 175-kDa protein, which is larger than the molecular weight for MRP4 (149 kDa) predicted from the sequence in the Swiss-Prot database. Deglycosylation of the cell lysates with N-glycosidase F resulted in a reduction in the molecular weight, suggesting that the molecular weight of MRP4 in the MRP4/CES1A1-expressing MDCKII cells was increased by glycosylation (Fig. 1B).

Efflux of Ro 64-0802 formed intracellularly from oseltamivir in human GFP/CES1A1 and MRP4/CES1A1-expressing MDCKII cells

An efflux transport experiment was conducted using MRP4/CES1A1- and GFP/CES1A1-MDCKII cells. When MRP4/CES1A1- and GFP/CES1A1-MDCKII were incubated with oseltamivir, Ro 64-0802 was detected in both the buffer and the cells in a time-dependent manner (Fig. 1C and 1D). The concentration of Ro 64-0802 in the buffer was higher for the MRP4/CES1A1-MDCKII cells than for the GFP/CES1A1-MDCKII cells, and cellular Ro 64-0802 was lower in the MRP4/CES1A1-MDCKII cells (Fig. 1C and 1D). Indomethacin, an inhibitor of MRP4 (Reid et al., 2003; Nozaki et al., 2007), reversed the effects of exogenous MRP4 expression.

Integration plots of the efflux transport of Ro 64-0802 are shown in Fig. 2A. The efflux clearance of Ro 64-0802 from MRP4/CES1A1-MDCKII cells was 3.1-fold greater than that from GFP/CES1A1-MDCKII cells and was significantly inhibited by indomethacin (Fig. 2B).

Efflux of Ro 64-0802 from the cerebral cortex of wild-type and *Oat3*^{-/-} mice following microinjection

Real-time PCR was performed to check the adaptive regulation of efflux transporters at the BBB of *Oat3*^{-/-} mice. There were no significant differences in the mRNA expression of Mdr1a, Bcrp, Mrp4, Organic anion transporter peptide 1a4 (*Oatp1a4*), or *Oatp1c1* in the cerebral cortex, quantified by real-time PCR, between wild-type and *Oat3*^{-/-} mice (data not shown).

To examine the involvement of *Oat3* in the efflux transport of Ro 64-0802 across the BBB, Ro 64-0802 was directly injected into the mouse cerebral cortex, and the amount of Ro 64-0802 remaining in the brain was determined at 60 and 120 min after injection. The amount of Ro 64-0802 remaining in the brain was compared between wild-type and *Oat3*^{-/-} mice (Fig. 3). As shown in Fig. 3, *Oat3*^{-/-} mice exhibited delayed elimination of Ro 64-0802 from the brain compared with that in wild-type mice.

Efflux of Ro 64-0802 from the cerebral cortex of wild-type and *Mrp4*^{-/-} mice following microinjection

Real-time PCR was used to check the adaptive regulation of efflux transporters at the BBB of *Mrp4*^{-/-} mice. No significant differences were observed in the mRNA expression levels of Mdr1a, Bcrp, *Oat3*, *Oatp1a4*, or *Oatp1c1* in the cerebral cortex, quantified by real-time PCR, between wild-type and *Mrp4*^{-/-} mice. (data not shown).

To examine the involvement of *Mrp4* in the efflux transport of Ro 64-0802 across the BBB, Ro 64-0802 was directly injected into the mouse cerebral cortex, and the amount of Ro 64-0802 remaining in the brain was determined at 60 and 120 min after injection. The amount of Ro 64-0802 remaining in the brain was compared between wild-type and *Mrp4*^{-/-} mice (Fig. 4). As shown in Fig.

4, *Mrp4*^{-/-} mice exhibited delayed elimination of Ro 64-0802 from the brain compared with that in wild-type mice.

Brain-to-plasma concentration ratio of Ro 64-0802 following subcutaneous infusion of oseltamivir or Ro 64-0802 in wild-type, *Oat3*^{-/-} and *Mrp4*^{-/-} mice

To clarify the importance of the *Oat3*- and *Mrp4*-mediated efflux of Ro 64-080 at the BBB, Ro 64-080 was given to mice by subcutaneous infusion for 24 h, and the $K_{p,brain}$ of Ro 64-0802 was determined. The concentrations of Ro 64-080 in the plasma were 4.5 ± 0.6 and 4.5 ± 1.3 μ M in wild-type and *Oat3*^{-/-} mice, respectively. The $K_{p,brain}$ of Ro 64-0802 in *Oat3*^{-/-} mice was not significantly different from that in wild-type mice and remained close to the capillary volume in the brain (Fig. 5). After subcutaneous infusions of oseltamivir in wild-type or *Mrp4*^{-/-} mice, the plasma concentrations of Ro 64-0802 were 6.9 ± 2.3 and 12 ± 5 μ M, respectively. The $K_{p,brain}$ of Ro 64-0802 was 3.8-fold higher in *Mrp4*^{-/-} mice than that in wild-type mice (Fig. 6). Even after subcutaneous infusions of Ro 64-0802, the $K_{p,brain}$ of Ro 64-0802 was a 6.4-fold greater in *Mrp4*^{-/-} mice than that in wild-type mice (Fig. 6). The plasma concentrations of Ro 64-0802 were 5.7 ± 0.8 and 3.8 ± 1.7 μ M in wild-type and *Mrp4*^{-/-} mice treated with Ro 64-0802, respectively.

Discussion

Abnormal behavior is a suspected adverse effect of oseltamivir on the central nervous system. To understand the pharmacological action of oseltamivir in the brain, its uptake and efflux transport across the BBB were investigated as factors that determine its exposure to the central nervous system. In this study, we focused on Oat3 and Mrp4 as transporters of Ro 64-0802, a pharmacologically active form of oseltamivir, across the BBB.

Firstly, we examined the involvement of Oat3 in the elimination of Ro 64-0802 from the cerebral cortex following microinjection because an in vitro transport study using OAT3-expressing HEK cells identified Ro 64-0802 as a substrate of OAT3. The elimination of Ro 64-0802 from the brain after its microinjection into the cerebral cortex was markedly delayed in *Oat3*^{-/-} mice compared with wild-type mice (Fig. 3). This suggests that Oat3 plays a significant role in the efflux of Ro 64-0802 from the brain by facilitating its uptake from the brain interstitial space to endothelial cells. For the directional efflux of Ro 64-0802 from the brain to the blood across the BBB, a transporter(s) is also required to facilitate its luminal efflux, considering the hydrophilic nature of Ro 64-0802. Previously, we demonstrated that the brain concentrations of Ro 64-0802 in *Mdr1a/1b*^{-/-} and *Abcg2*^{-/-} mice are similar to that in wild-type mice (Ose et al., 2008), excluding the possibility that P-gp and Bcrp are involved in the luminal efflux of Ro 64-0802. Therefore, we focused on Mrp4, another ABC transporter at the BBB, as a candidate transporter because it has been reported to mediate the active efflux of topotecan and adefovir across the BBB (Leggas et al., 2004; Belinsky et al., 2007). To show that Ro 64-0802 is a substrate of MRP4, we constructed double transfectant cells expressing both CES1A1, an enzyme producing Ro 64-0802 from oseltamivir, and MRP4 (MRP4/CES1A1-MDCKII). The double transfectant exhibited enhanced efflux of Ro 64-0802 (which was inhibited by an MPR4 inhibitor, indomethacin) compared with GFP/CES1A1-MDCKII (Fig. 2B). It should be noted that the host cells also exhibited indomethacin-sensitive efflux of Ro 64-0802. This is presumably attributable to endogenous canine MRP4 because its mRNA expression was detected by reverse transcription-PCR in MDCKII cells (data not shown). The involvement of Mrp4 in the efflux of Ro 64-0802 across the BBB was then examined using *Mrp4*^{-/-} mice by

microinjection into the cerebral cortex. *Mrp4*^{-/-} mice exhibited delayed elimination of Ro 64-0802 from the cerebral cortex after its microinjection compared with that in wild-type mice (Fig. 4). Therefore, Mrp4 plays an important role in the luminal efflux of Ro 64-0802 after its cellular uptake by Oat3 from the brain side.

To show the importance of the active efflux of Ro 64-0802 at the BBB mediated by Oat3 and Mrp4, the $K_{p,brain}$ of Ro 64-0802 was determined in *Oat3*^{-/-} or *Mrp4*^{-/-} mice given Ro 64-0802 by subcutaneous infusion for 24 h. Our approach was based on the pharmacokinetic concept that reduced efflux across the BBB may lead to an increase in the $K_{p,brain}$. Consistent with a previous report (Ose et al., 2008), the $K_{p,brain}$ of Ro 64-0802 was close to the capillary volume in wild-type mice. The $K_{p,brain}$ of Ro 64-0802 observed in *Oat3*^{-/-} mice was also close to the capillary volume (Fig. 5). In contrast, the $K_{p,brain}$ of Ro 64-0802 was 4-6-fold greater in *Mrp4*^{-/-} mice than that in wild-type mice receiving either oseltamivir or Ro 64-0802 (Fig. 6). These *in vivo* results using *Mrp4*^{-/-} mice thus indicate that Ro 64-0802 crosses the BBB from the blood side to the brain, but Mrp4 limits its penetration into the brain by extruding it into the blood. The latter finding is consistent with the results of our microinjection experiment. However, the lack of effect of knockout of *Oat3* on the $K_{p,brain}$ of Ro 64-0802 seems to contradict the results of the microinjection experiment. There are three explanations for this discrepancy. The first explanation is that luminal Mrp4 is more important in preventing brain penetration than abluminal Oat3. The second explanation is that, considering Oat3 mediates bidirectional transport (Bakhiya et al., 2003), it is possible that Oat3 on the abluminal membrane of brain endothelial cells may act in the efflux of Ro 64-0802 from inside the endothelial cells into the brain, as well as in its uptake from the brain to the endothelial cells (Fig. 7). The third explanation is that, considering the hydrophilic character of Ro 64-0802, with an anionic charge, its luminal uptake probably involves transporters. Kikuchi et al. suggested that Oat3 is expressed on both the luminal and abluminal membranes of rat brain capillaries (Kikuchi et al., 2003), however this localization is controversial (Mori et al., 2003; Roberts et al., 2008). Oat3 may serve as an uptake system for Ro 64-0802 on the luminal membrane from the circulating blood into the brain

(Fig.7). Further studies using *Mrp4* and *Oat3* double knockout mice can answer these questions and perhaps confirm these speculations.

Figure 7 summarizes the proposed mechanisms determining the brain distribution of oseltamivir and Ro 64-0802 in humans. P-gp, MRP4, and CES1A1 are factors that determine the brain distribution of oseltamivir and Ro 64-0802 in humans. CES1A1 is predominantly expressed in the brain capillaries in human brain (Yamada et al., 1994), although whether CES1A1 is the only enzyme responsible for the conversion of oseltamivir remains to be examined. MRP4 is also expressed on the luminal membranes of human brain capillaries (Nies et al., 2004; Bronger et al., 2005). Because oseltamivir crosses the BBB, Ro 64-0802 can be produced during the penetration of oseltamivir across the BBB and then subjected to active efflux by MRP4. Although northern blotting did detect OAT3 mRNA expression in the human brain (Cha et al., 2001), its distribution and membrane localization remain to be determined. Therefore, whether Ro 64-0802 can penetrate into the brain and is eliminated from the brain by OAT3 in humans, as well as in mice, also remains in question. Fluctuations in their activities will cause interindividual variations in their exposure to the central nervous system. For instance, genetic variations have been reported for P-gp and MRP4, which may alter their transport activities and expression. The silent mutation 3435C>T is associated with reduced P-gp expression (Hoffmeyer et al., 2000) and affects protein folding, resulting in a substrate-dependent functional change (Kimchi-Sarfaty et al., 2007). In MRP4, the nonsynonymous mutations 559G>T, 1460G>A, and 2269G>A are associated with altered transport activity and expression (Abla et al., 2008; Krishnamurthy et al., 2008). It is possible that these polymorphisms are associated with the adverse effects of Ro 64-0802 on the central nervous system.

In conclusion, *Mrp4* and *Oat3* are responsible for the elimination of Ro 64-0802 from the brain across the BBB although, at steady-state, *Oat3* may not affect its brain distribution, probably because of its possible contribution also to the brain uptake of Ro 64-0802. This is the first demonstration of the cooperation of uptake and efflux transporters in the directional (brain-to-blood) transport of anionic drugs across the BBB.

Acknowledgments

The authors thank Dr. Junko Iida and Futoshi Kurotobi (Shimadzu Corporation, Kyoto, Japan) for their technical support with the LC–MS system.

References

- Abla N, Chinn LW, Nakamura T, Liu L, Huang CC, Johns SJ, Kawamoto M, Stryke D, Taylor TR, Ferrin TE, Giacomini KM and Kroetz DL (2008) The human multidrug resistance protein 4 (MRP4, ABCC4): functional analysis of a highly polymorphic gene. *J Pharmacol Exp Ther* **325**:859-868.
- Bakhiya A, Bahn A, Burckhardt G and Wolff N (2003) Human organic anion transporter 3 (hOAT3) can operate as an exchanger and mediate secretory urate flux. *Cell Physiol Biochem* **13**:249-256.
- Bardsley-Elliot A and Noble S (1999) Oseltamivir. *Drugs* **58**:851-860; discussion 861-852.
- Belinsky MG, Guo P, Lee K, Zhou F, Kotova E, Grinberg A, Westphal H, Shchaveleva I, Klein-Szanto A, Gallo JM and Kruh GD (2007) Multidrug resistance protein 4 protects bone marrow, thymus, spleen, and intestine from nucleotide analogue-induced damage. *Cancer Res* **67**:262-268.
- Bronger H, Konig J, Kopplow K, Steiner HH, Ahmadi R, Herold-Mende C, Keppler D and Nies AT (2005) ABC drug efflux pumps and organic anion uptake transporters in human gliomas and the blood-tumor barrier. *Cancer Res* **65**:11419-11428.
- Cha SH, Sekine T, Fukushima JI, Kanai Y, Kobayashi Y, Goya T and Endou H (2001) Identification and characterization of human organic anion transporter 3 expressing predominantly in the kidney. *Mol Pharmacol* **59**:1277-1286.
- Ci L, Kusuhara H, Adachi M, Schuetz JD, Takeuchi K and Sugiyama Y (2007) Involvement of MRP4 (ABCC4) in the luminal efflux of ceftizoxime and cefazolin in the kidney. *Mol Pharmacol* **71**:1591-1597.
- Deguchi T, Kusuhara H, Takadate A, Endou H, Otagiri M and Sugiyama Y (2004) Characterization of uremic toxin transport by organic anion transporters in the kidney. *Kidney Int* **65**:162-174.
- Fuyuno I (2007) Tamiflu side effects come under scrutiny. *Nature* **446**:358-359.
- Hasegawa M, Kusuhara H, Adachi M, Schuetz JD, Takeuchi K and Sugiyama Y (2007) Multidrug resistance-associated protein 4 is involved in the urinary excretion of hydrochlorothiazide and furosemide. *J Am Soc Nephrol* **18**:37-45.
- He G, Massarella J and Ward P (1999) Clinical pharmacokinetics of the prodrug oseltamivir and its active metabolite Ro 64-0802. *Clin Pharmacokinet* **37**:471-484.
- Hill G, Cihlar T, Oo C, Ho ES, Prior K, Wiltshire H, Barrett J, Liu B and Ward P (2002) The anti-influenza drug oseltamivir exhibits low potential to induce pharmacokinetic drug interactions via renal secretion-correlation of in vivo and in vitro studies. *Drug Metab Dispos* **30**:13-19.
- Hoffmeyer S, Burk O, von Richter O, Arnold HP, Brockmoller J, John A, Cascorbi I, Gerloff T, Roots I, Eichelbaum M and Brinkmann U (2000) Functional polymorphisms of the human multidrug-resistance gene: multiple sequence variations and correlation of one allele with P-glycoprotein expression and activity in vivo. *Proc Natl Acad Sci U S A* **97**:3473-3478.
- Imaoka T, Kusuhara H, Adachi M, Schuetz JD, Takeuchi K and Sugiyama Y (2007) Functional involvement of multidrug resistance-associated protein 4 (MRP4/ABCC4) in the renal elimination of the antiviral drugs adefovir and tenofovir. *Mol Pharmacol* **71**:619-627.
- Izumi Y, Tokuda K, O'Dell K A, Zorumski CF and Narahashi T (2007) Neuroexcitatory actions of Tamiflu and its carboxylate metabolite. *Neurosci Lett* **426**:54-58.
- Kakee A, Terasaki T and Sugiyama Y (1996) Brain efflux index as a novel method of analyzing efflux transport at the blood-brain barrier. *J Pharmacol Exp Ther* **277**:1550-1559.
- Kikuchi R, Kusuhara H, Abe T, Endou H and Sugiyama Y (2004) Involvement of multiple transporters in the efflux of 3-hydroxy-3-methylglutaryl-CoA reductase inhibitors across the blood-brain barrier. *J Pharmacol Exp Ther* **311**:1147-1153.
- Kikuchi R, Kusuhara H, Sugiyama D and Sugiyama Y (2003) Contribution of organic anion transporter 3 (Slc22a8) to the elimination of p-aminohippuric acid and benzylpenicillin across the blood-brain barrier. *J Pharmacol Exp Ther* **306**:51-58.

- Kimchi-Sarfaty C, Oh JM, Kim IW, Sauna ZE, Calcagno AM, Ambudkar SV and Gottesman MM (2007) A "silent" polymorphism in the MDR1 gene changes substrate specificity. *Science* **315**:525-528.
- Krishnamurthy P, Schwab M, Takenaka K, Nachagari D, Morgan J, Leslie M, Du W, Boyd K, Cheok M, Nakauchi H, Marzolini C, Kim RB, Poonkuzhali B, Schuetz E, Evans W, Relling M and Schuetz JD (2008) Transporter-mediated protection against thiopurine-induced hematopoietic toxicity. *Cancer Res* **68**:4983-4989.
- Leggas M, Adachi M, Scheffer GL, Sun D, Wielinga P, Du G, Mercer KE, Zhuang Y, Panetta JC, Johnston B, Scheper RJ, Stewart CF and Schuetz JD (2004) Mrp4 confers resistance to topotecan and protects the brain from chemotherapy. *Mol Cell Biol* **24**:7612-7621.
- Lindegardh N, Davies GR, Tran TH, Farrar J, Singhasivanon P, Day NP and White NJ (2006) Rapid degradation of oseltamivir phosphate in clinical samples by plasma esterases. *Antimicrob Agents Chemother* **50**:3197-3199.
- Mori M, Hosokawa M, Ogasawara Y, Tsukada E and Chiba K (1999) cDNA cloning, characterization and stable expression of novel human brain carboxylesterase. *FEBS Lett* **458**:17-22.
- Mori S, Ohtsuki S, Takanaga H, Kikkawa T, Kang YS and Terasaki T (2004) Organic anion transporter 3 is involved in the brain-to-blood efflux transport of thiopurine nucleobase analogs. *J Neurochem* **90**:931-941.
- Mori S, Takanaga H, Ohtsuki S, Deguchi T, Kang YS, Hosoya K and Terasaki T (2003) Rat organic anion transporter 3 (rOAT3) is responsible for brain-to-blood efflux of homovanillic acid at the abluminal membrane of brain capillary endothelial cells. *J Cereb Blood Flow Metab* **23**:432-440.
- Morimoto K, Nakakariya M, Shirasaka Y, Kakinuma C, Fujita T, Tamai I and Ogihara T (2008) Oseltamivir (Tamiflu) efflux transport at the blood-brain barrier via P-glycoprotein. *Drug Metab Dispos* **36**:6-9.
- Nies AT, Jedlitschky G, Konig J, Herold-Mende C, Steiner HH, Schmitt HP and Keppler D (2004) Expression and immunolocalization of the multidrug resistance proteins, MRP1-MRP6 (ABCC1-ABCC6), in human brain. *Neuroscience* **129**:349-360.
- Nozaki Y, Kusuvara H, Kondo T, Iwaki M, Shiroyanagi Y, Nakayama H, Horita S, Nakazawa H, Okano T and Sugiyama Y (2007) Species difference in the inhibitory effect of nonsteroidal anti-inflammatory drugs on the uptake of methotrexate by human kidney slices. *J Pharmacol Exp Ther* **322**:1162-1170.
- Ohtsuki S, Asaba H, Takanaga H, Deguchi T, Hosoya K, Otagiri M and Terasaki T (2002) Role of blood-brain barrier organic anion transporter 3 (OAT3) in the efflux of indoxyl sulfate, a uremic toxin: its involvement in neurotransmitter metabolite clearance from the brain. *J Neurochem* **83**:57-66.
- Ose A, Kusuvara H, Yamatsugu K, Kanai M, Shibasaki M, Fujita T, Yamamoto A and Sugiyama Y (2008) P-glycoprotein restricts the penetration of oseltamivir across the blood-brain barrier. *Drug Metab Dispos* **36**:427-434.
- Reid G, Wielinga P, Zelcer N, van der Heijden I, Kuil A, de Haas M, Wijnholds J and Borst P (2003) The human multidrug resistance protein MRP4 functions as a prostaglandin efflux transporter and is inhibited by nonsteroidal antiinflammatory drugs. *Proc Natl Acad Sci U S A* **100**:9244-9249.
- Roberts LM, Black DS, Raman C, Woodford K, Zhou M, Haggerty JE, Yan AT, Cwirla SE and Grindstaff KK (2008) Subcellular localization of transporters along the rat blood-brain barrier and blood-cerebral-spinal fluid barrier by in vivo biotinylation. *Neuroscience*.
- Satoh K, Nonaka R, Ogata A, Nakae D and Uehara S (2007) Effects of oseltamivir phosphate (Tamiflu) and its metabolite (GS4071) on monoamine neurotransmission in the rat brain. *Biol Pharm Bull* **30**:1816-1818.
- Shi D, Yang J, Yang D, LeCluyse EL, Black C, You L, Akhlaghi F and Yan B (2006) Anti-influenza prodrug oseltamivir is activated by carboxylesterase human carboxylesterase 1, and the activation is inhibited by antiplatelet agent clopidogrel. *J Pharmacol Exp Ther* **319**:1477-1484.

- Usami A, Sasaki T, Satoh N, Akiba T, Yokoshima S, Fukuyama T, Yamatsugu K, Kanai M, Shibasaki M, Matsuki N and Ikegaya Y (2008) Oseltamivir enhances hippocampal network synchronization. *J Pharmacol Sci* **106**:659-662.
- Wiltshire H, Wiltshire B, Citron A, Clarke T, Serpe C, Gray D and Herron W (2000) Development of a high-performance liquid chromatographic-mass spectrometric assay for the specific and sensitive quantification of Ro 64-0802, an anti-influenza drug, and its pro-drug, oseltamivir, in human and animal plasma and urine. *J Chromatogr B Biomed Sci Appl* **745**:373-388.
- Yamada T, Hosokawa M, Satoh T, Moroo I, Takahashi M, Akatsu H and Yamamoto T (1994) Immunohistochemistry with an antibody to human liver carboxylesterase in human brain tissues. *Brain Res* **658**:163-167.
- Yamaoka K, Tanigawara Y, Nakagawa T and Uno T (1981) A pharmacokinetic analysis program (multi) for microcomputer. *J Pharmacobiodyn* **4**:879-885.
- Yamatsugu K, Kamijo S, Suto Y, Kanai M and Shibasaki M (2007) A concise synthesis of Tamiflu: third generation route via the Diels-Alder reaction and the Curtius rearrangement. *Tetrahedron Lett* **48**:1403-1406.
- Yoshino T, Nisijima K, Shioda K, Yui K and Kato S (2008) Oseltamivir (Tamiflu) increases dopamine levels in the rat medial prefrontal cortex. *Neurosci Lett* **438**:67-69.

Footnotes

This work was partly supported by Health and Labor Sciences Research Grants from the Grant-in-Aid for Scientific Research (A) (20249008 to Y.S.), and Scientific Research (B) (20390046 to H.K.) from the Ministry of Education, Culture, Sports, Science and Technology (MEXT).

Figure legends

Fig. 1. Efflux of intracellularly formed Ro 64-0802 from mock-transfected and MRP4-expressing MDCKII cells

(A-B) Western blotting: Cell lysates were prepared from mock-transfected (GFP/CES1A1-MDCKII) and MRP4-expressing MDCKII cells (MRP4/CES1A1-MDCKII) and subjected to SDS-PAGE (7.5%) (A). N-Linked carbohydrate groups were cleaved from the MRP4 protein in the cell lysates using PNGase F (N-glycosidase F) (B). MRP4 was detected by the monoclonal anti-MRP4 M4I-10 antibody. (C-D) Efflux transport study: MRP4/CES1A1-MDCKII (closed symbols) and GFP/CES1A1-MDCKII cells (open symbols) were incubated with 10 μ M oseltamivir in the presence (triangles) or absence (circles) of indomethacin (50 μ M) at 37 °C. Each point represents the mean \pm SE (n = 6). Statistical significance was calculated by one-way ANOVA followed by Tukey's multiple comparison test. * P < 0.05, ** P < 0.01, *** P < 0.001, significantly different between MRP4/CES1A1-MDCKII and GFP/CES1A1-MDCKII cells. ## P < 0.01, ### P < 0.001, significantly different in GFP/CES1A1-MDCKII cells with and without indomethacin. ++ P < 0.01, +++ P < 0.001, significantly different in MRP4/CES1A1-MDCKII cells with and without indomethacin.

Fig. 2. Integration plots of the efflux transport of Ro 64-0802 from MRP4/CES1A1-MDCKII and GFP/CES1A1-MDCKII cells

(A) Integration plot: The amount of Ro 64-0802 in buffer ($A_{\text{buffer}}(t)$) was plotted against $AUC_{\text{cell}}(0-t)$ in MRP4/CES1A1-MDCKII (closed symbols) and GFP/CES1A1-MDCKII cells (open symbols) in the presence (triangles) or absence (circles) of indomethacin (50 μ M). The data used for the calculation are cited in Fig. 1C-D. The slope of the plot represents the efflux clearance. Each point represents a mean \pm SE (n = 6). (B) Efflux clearance of Ro 64-0802: The efflux clearance of Ro 64-0802 was calculated from the slope of the integration plot (panel A). Statistical significance was calculated by one-way ANOVA followed by Tukey's multiple comparison test. *** P < 0.001, significantly different between MRP4/CES1A1-MDCKII and GFP/CES1A1-MDCKII cells. ††† P <

0.001, significantly different efflux clearance in the presence and absence of indomethacin. Data represent means \pm computer calculated SD ($\mu\text{L}/\text{min}$ per mg protein).

Fig. 3. Comparison of the amounts of Ro 64-0802 in the ipsilateral cerebrum after intracerebral microinjection of Ro 64-0802 in wild-type mice and *Oat3*^{-/-} mice

Ro 64-0802 (1 mM) in 0.5 μL of ECF buffer was injected into the Par2 region (4.5 mm lateral to the bregma, 2.5 mm in depth). The amount of Ro 64-0802 in the ipsilateral cerebrum was determined at 60 and 120 min after treatment. The data for wild-type and *Oat3*^{-/-} mice are shown as open and closed bars, respectively. Each bar represents the mean \pm SE (n = 3–4). Asterisks represent statistically significant differences between wild-type and *Oat3*^{-/-} mice, **P* < 0.05 and ****P* < 0.001.

Fig. 4. Comparison of the amounts of Ro 64-0802 in the ipsilateral cerebrum after intracerebral microinjection of Ro 64-0802 in wild-type mice and *Mrp4*^{-/-} mice

Ro 64-0802 (1 mM) in 0.5 μL of ECF buffer was injected into the Par2 region (4.5 mm lateral to the bregma, 2.5 mm in depth). The amount of Ro 64-0802 in the ipsilateral cerebrum was determined at 60 and 120 min after treatment. The data for the wild-type and *Mrp4*^{-/-} mice are shown as open and closed bars, respectively. Each bar represents the mean \pm SE (n = 3–4). Asterisks represent statistically significant differences between wild-type and *Mrp4*^{-/-} mice, ***P* < 0.01 and ****P* < 0.001.

Fig. 5. Comparison of the brain-to-plasma concentration ratio ($K_{p,\text{brain}}$) of Ro 64-0802 following subcutaneous infusion of Ro 64-0802 in wild-type mice and *Oat3*^{-/-} mice

Mice received a continuous subcutaneous infusion of Ro 64-0802 at a dose of 80 nmol/h per mouse for 24 h, with an osmotic pump. The plasma and brain concentrations of Ro 64-0802 were determined at 24 h after treatment. The data for wild-type mice are shown as open bars, and those for *Oat3*^{-/-} mice as closed bars. Each bar represents the mean \pm SE (n = 3–4).

Fig. 6. Comparison of the brain-to-plasma concentration ratio ($K_{p,\text{brain}}$) of Ro 64-0802 following subcutaneous infusion of either oseltamivir or Ro 64-0802 in wild-type mice and *Mrp4*^{-/-} mice

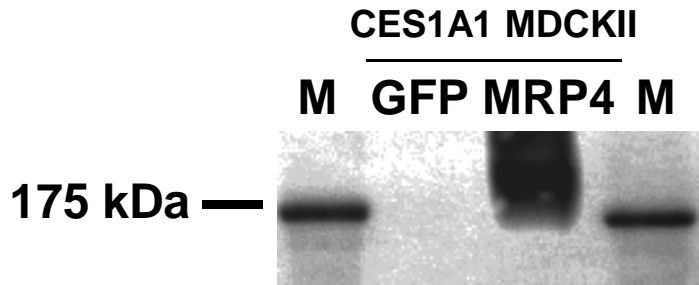
Mice received a continuous subcutaneous infusion of either oseltamivir or Ro 64-0802 at a dose of 400 or 80 nmol/h per mouse, respectively, for 24 h with an osmotic pump. The plasma and brain concentrations of Ro 64-0802 were determined at 24 h after treatment. The data for the wild-type and *Mrp4*^{-/-} mice are shown as open and closed bars, respectively. Each bar represents the mean ± SE (n = 4–6). Asterisks represent statistically significant differences between wild-type and *Mrp4*^{-/-} mice, ***P* < 0.01 and ****P* < 0.001.

Fig. 7. Schematic representation of the proposed mechanism underlying the brain distribution of oseltamivir and Ro 64-0802 in humans

Oseltamivir crosses the BBB, and Ro 64-0802 is produced by CES1A1 during the penetration of oseltamivir across the BBB. Both oseltamivir and Ro 64-0802 are subjected to active efflux by P-gp and MRP4, respectively. The functional importance of OAT3 at the human BBB has not yet been established, so the hypothetical pathway is shown with a broken line.

Fig. 1

(A)



(B)

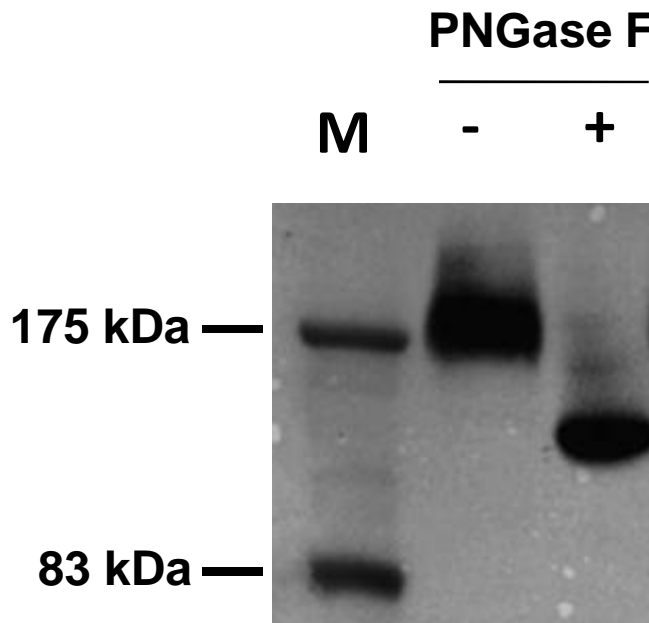
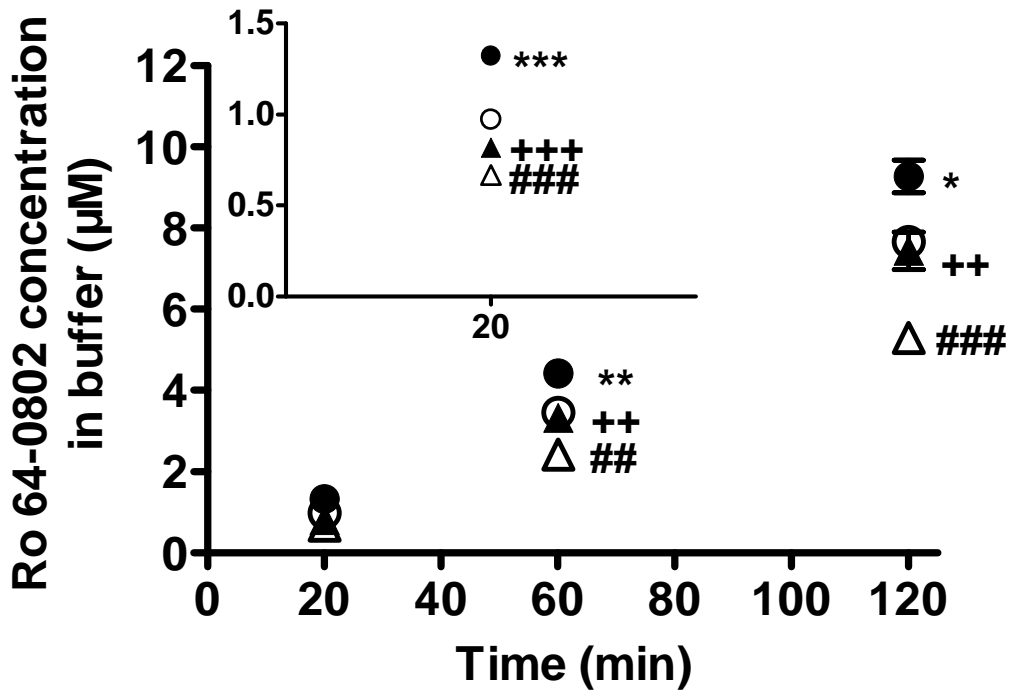


Fig. 1 (continued)

(C) Concentration in buffer



(D) Cellular amount

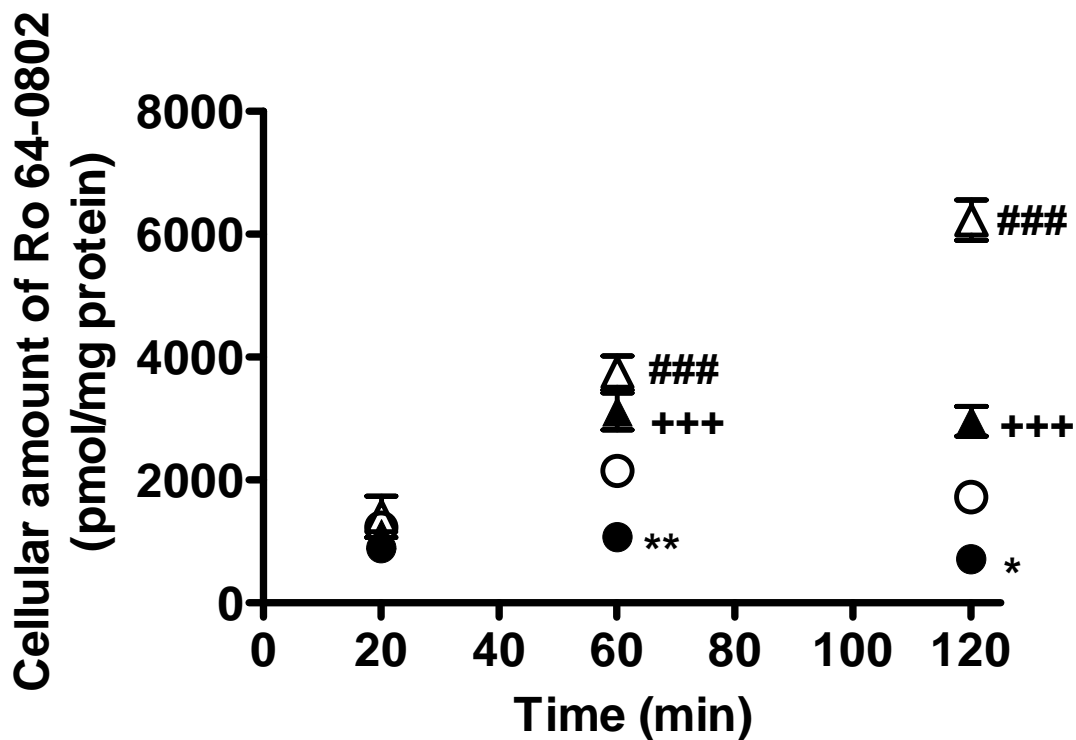


Fig. 2

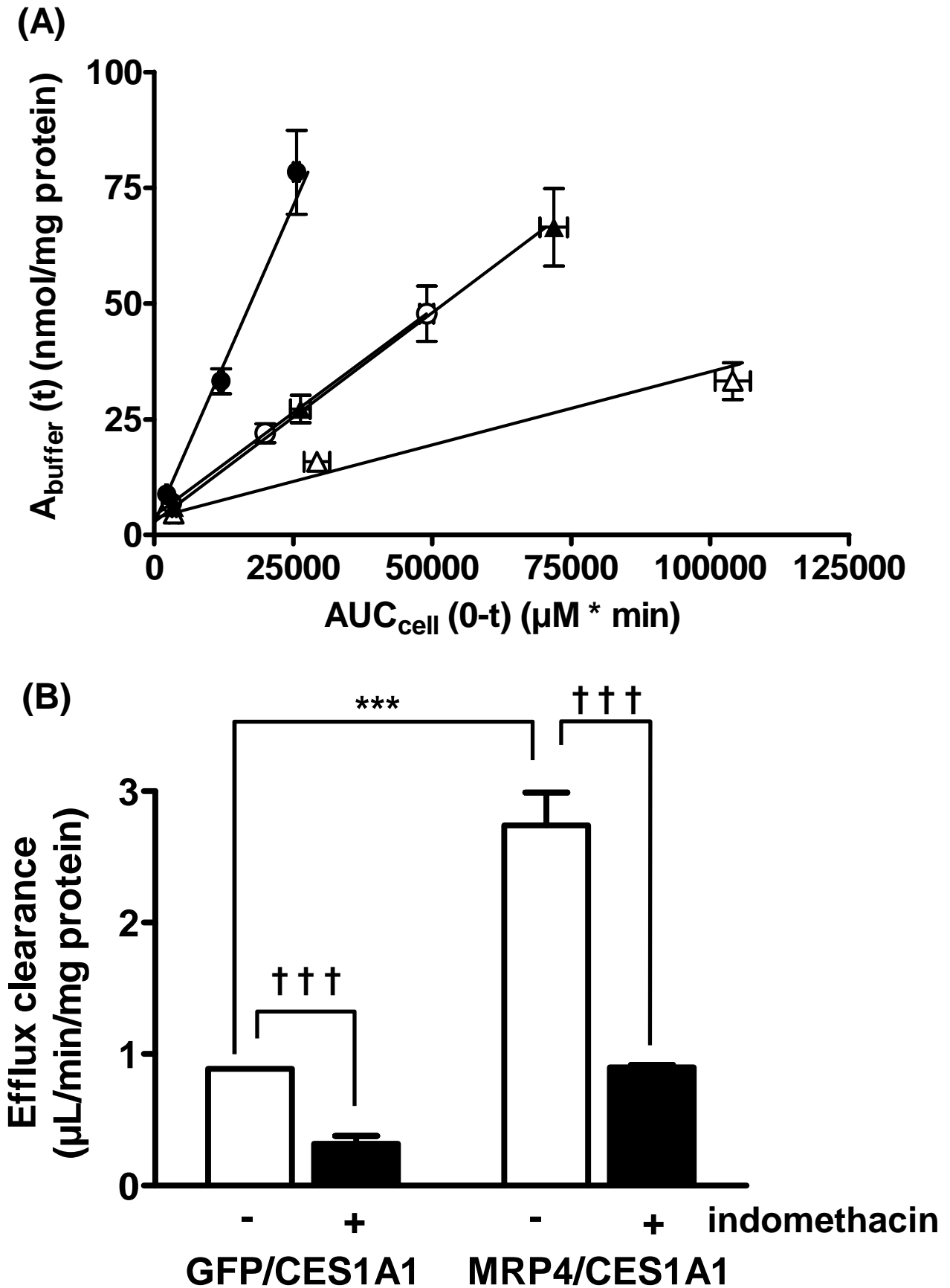


Fig. 3

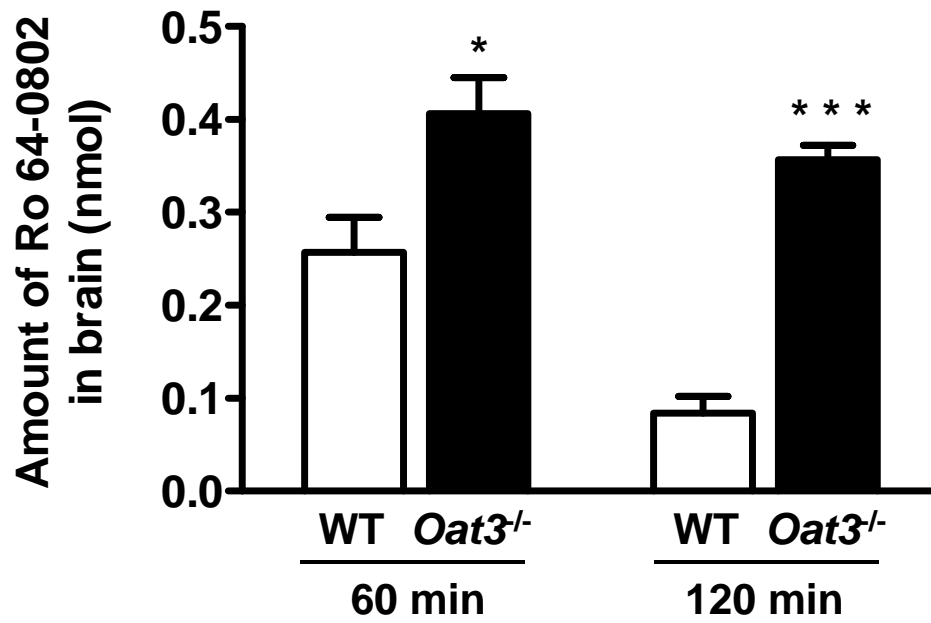


Fig. 4

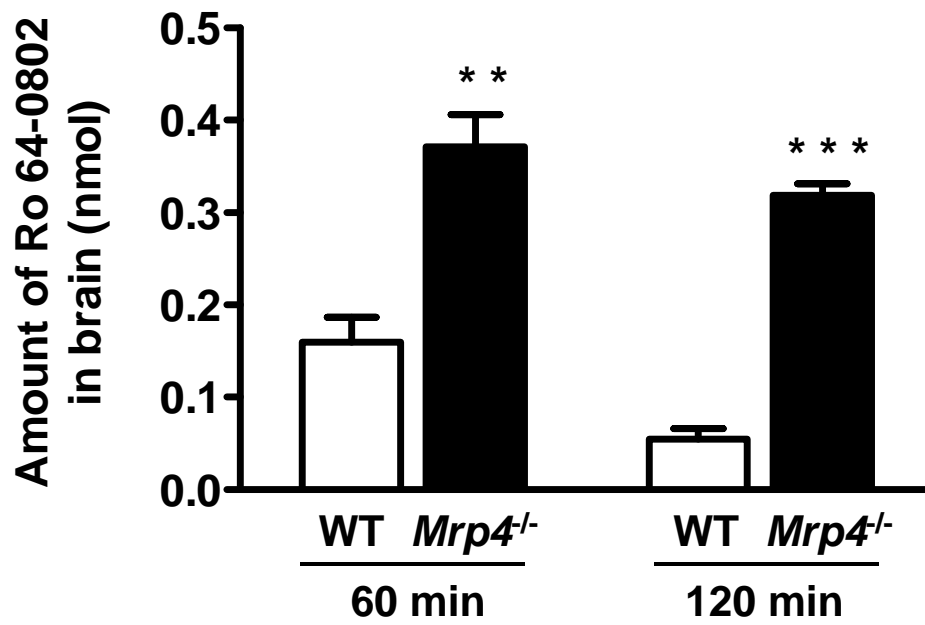


Fig. 5

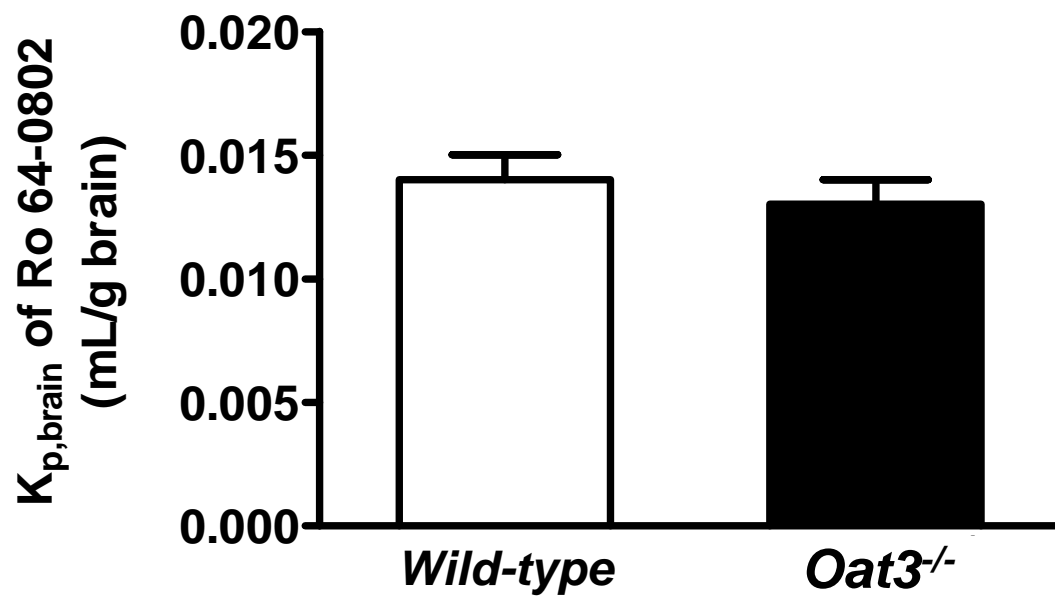


Fig. 6

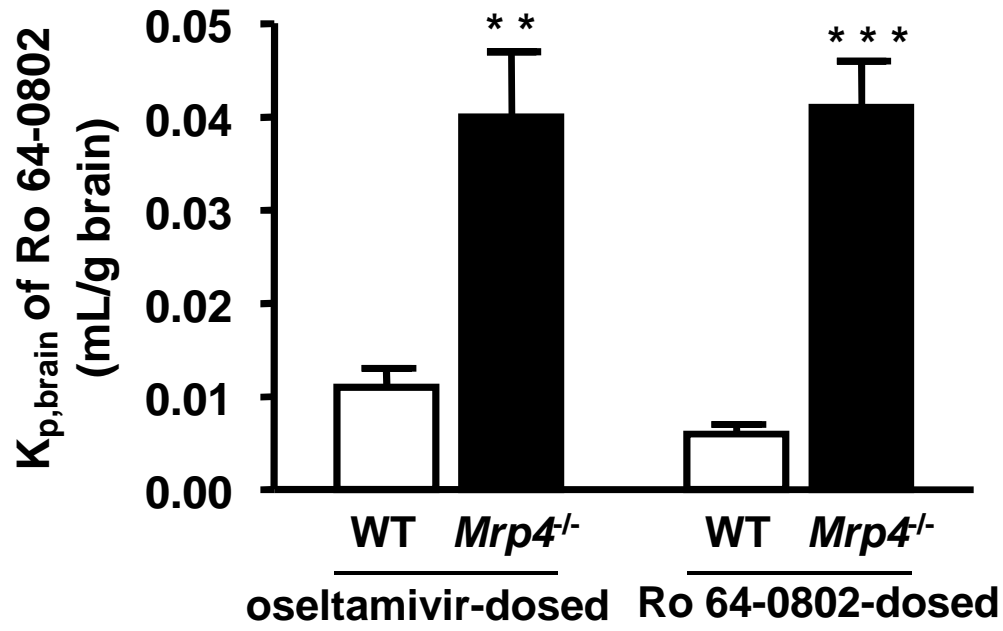


Fig. 7

